Defence Science Journal, Vol. 73, No. 3, May 2023, pp. 313-321, DOI : 10.14429/dsj.73.18342

Estimation of Trajectory of High-Speed Artillery Shell

Manoj Sharma[#,*] and Subrat Kar[$]

[#]*DRDO-Directorate of Information Technology and Cyber Security, DRDO Hqrs, New Delhi - 110 011, India*
[$]*Department of Electrical Engineering, Indian Institute of Technology, New Delhi - 110016, India*
[*]*E-mail: manoj.hqr@gov.in*

ABSTRACT

This paper presents a novel technique that uses the stereoscopic arrangement of multiple cameras to determine the trajectory of a high-speed projectile. It can be used to detect and track artillery shells moving at high speed in the air toward friendly territory. A system with the proposed concept can enhance retaliation success in battlefield countermeasures. There are many state-of-the-art Radar-based systems to detect moving artillery shells and mortars, but the cost and size of those products make them not so easily deployable in all kinds of terrains. A system with multiple cameras is discussed in this paper as an alternative solution. The experimental results, after algorithms were applied to simulated videos of expected scenes showed that the proposed technique is feasible. The proposed technique is fast and accurate and can be converted into deployable hardware. It can lead to realizing a system that has utility in saving precious lives in critical circumstances.

Keywords: Counter battery fire; Artillery; Projectile; Tracking; Stereoscopic imaging; Trajectory; Geographic information system; Point of origin

1. INTRODUCTION

In artillery combat, often, the shelling starts from a point of origin that cannot be seen by the second party - for example, from behind a hillock mountain (reverse-slope). To retaliate effectively by counter-shelling, it is imperative that the counter-fire be directed exactly (a) at the point of origin of the enemy shell and (b) before the artillery gun is moved. Only the visual trajectory of the projectile is available to the unit under attack on the ground - so it is only based on this visually observed trajectory that we must accurately estimate the point of origin. In modern artillery, the artillery fire could be between 10 to 30 km away from the point of impact. Assuming a muzzle velocity of approximately 1000 m/s, the trajectory of the shell may be visible (in the air) for 2 to 5 sec from leaving the muzzle to impact.

Our problem, therefore, is this - from the visually observed trajectory of an incoming unpowered projectile *while it is in the air*, we need to estimate the point of origin (its latitude and longitude, with an accuracy of $\pm$ 50 m) of the projectile to direct the retaliatory counter-fire with maximum effect. The trajectory or flight path we observe while the shell is in the air is the only basis, we have to determine the possible point of origin (and the possible point of impact) given the geo-information of the area. From the partial flight path observed, we must estimate the entire flight path - the endpoints (point of origin and point of impact) and the trajectory. Determining the point of origin of the projectile is more crucial than finding the point of impact of the projectile - it allows immediate effective retaliation.

Received : 22 July 2022, Revised : 08 February 2023
Accepted : 21 February 2023, Online published : 12 May 2023

Measurement of real-world coordinates of the projectile as it travels at high speed in the air has to be accurate to precisely estimate the trajectory and eventually the point of origin. We propose multiple camera-based systems to sample the trajectory of the incoming shell visually using a system of N cameras (N$\geq$1). These samples are used by us to precisely estimate the point of origin of high-speed projectiles, e.g., artillery shells. With N=2, a pair of cameras (a minimal stereoscopic setup) is proposed to calculate the projectile's position in space while it is traveling at high speed. This pair of cameras is not without its limitations in tracking the projectile over a longer range as (a) their FOVs (Field of view) do not overlap completely and (b) using optics for a wider FOV, also reduces the resolution as the sensor inside the camera is fixed. We propose and present a novel design that uses multiple stereoscopic pairs to locate the position of a high-speed unpowered projectile (for example an artillery shell) over an extended range (by collecting a larger set of points in the visually tracked trajectory).

2. CHALLENGES

Calculating the trajectory of unpowered unguided projectiles has always interested scientists working in astronomy, defense, sports, and many others. There are existing solutions where radar systems with a high range of operation are used in defense and security to track projectiles from an unfriendly source[1-3]. Apart from being bulkier and costlier, these Radar-based systems are active systems and are prone to countermeasures as their signatures may also be known to adversaries. Work has been reported with the installation of cameras at multiple separated locations, which can extract information on the trajectory of meteors[4]. These multiple

cameras give the object's simultaneous spatial and temporal profile of interest. There is no literature available that can approve any completed or ongoing work around the proposed technique to measure the trajectory of high-speed shells, although similar techniques are used in sports for shorter ranges[5].

Figure 1 describes a situation where a shell is fired by artillery from a hidden source at A. The friendly territory is on the other side of the mountain terrain and contains point B where the shell is expected to drop and explode. We want to find the geo-coordinates of a hidden source at point-of-origin A by computing those coordinates from the world points (3-d points) through which the shell has moved. We propose a system that starts capturing the shell from a random point P1 measures its coordinates and then subsequent points (x_n, y_n, z_n), that lie on the path of the shell or projectile, at time instants t_n (for multiple points).

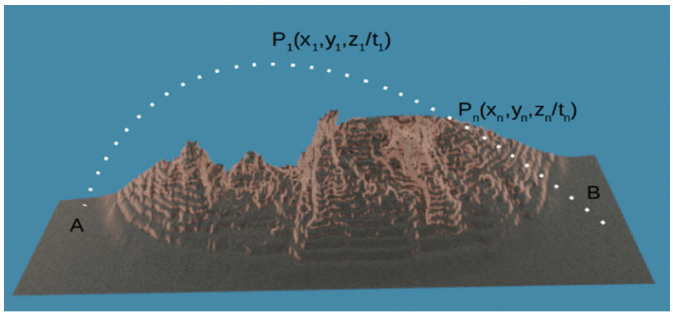

Figure 1. Artillery shell fired from a hidden source.

The proposed design considers the following three significant underlying challenges.

- **Speed of the artillery shell:** The artillery shell is expected to be traveling in the air with a net velocity between 100 m/s to 1000m/s[6-7]. Hence, computation on images to calculate parameters of interest must be fast, with a computational rate of 10 fps or even faster. A high frame rate is required for increased sampling to estimate an accurate trajectory.
- **Size of the artillery shell:** Projectiles fired by the hidden source can be of varying sizes. It can be challenging to detect it in the image from a larger distance. Our design must allow us to obtain a large number of samples of coordinates.
- **Distance of the source:** If the hidden source chooses to fire from a greater distance, it has to fire at a higher velocity, making the problem more difficult, as the distance from where the object must be tracked is larger and so is the projectile's speed. There is the issue of how the acquisition of the image is to be started, whether the camera must remain in continuous acquisition mode (i.e., acquire and discard frames constantly), or if image acquisition is to be auto-started based on some trigger such as the sound of the shell being fired. The speed of sound is a factor, and up to 3 seconds can be lost if the sound of firing is to be a trigger to initiate acquisition.

3. METHODOLOGY

We can consider what happens, on the ground, if there is only one camera whose field of view includes at least three points along with the trajectory - preferably one during ascent, peak, and descent each. Figure 2 illustrates that these three samples do not uniquely identify the trajectory. We can see that trajectories L, M, and N will have the "same measured points" though their points of origin are distinctly different.

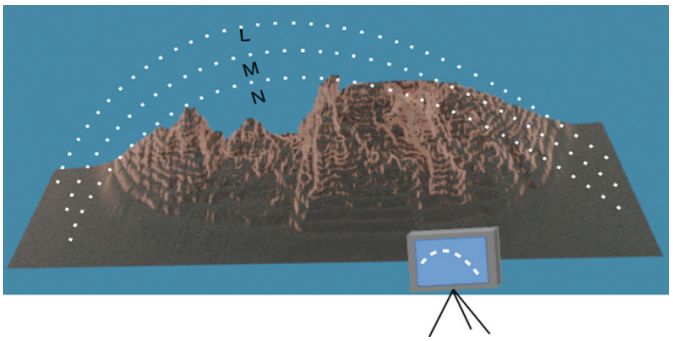

Figure 2. Single camera cannot identify the unique trajectory.

Therefore, we propose to use two cameras (stereoscopic) to determine the 3D trajectory uniquely. With two camera systems, the unique trajectory of the shell can be measured using the difference in pixel position of the projection of the world point on two cameras. One camera can map a set of trajectories to a single measured trajectory. Still, a stereoscope will lead to the estimation of a unique trajectory. Therefore, the system will be as shown in Fig. 3.

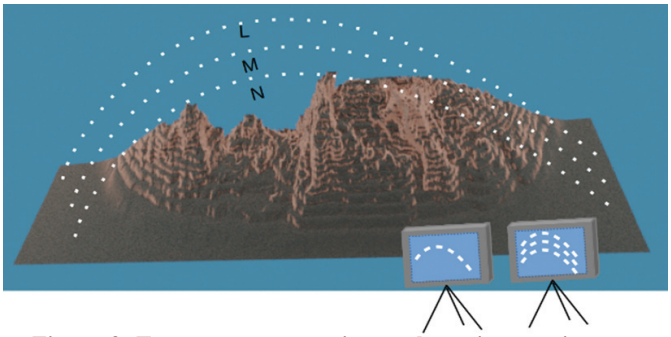

Figure 3. Two cameras to estimate the unique trajectory.

In a stereoscopic setup, we calculate the value of the world coordinates of the shell from several samples of its observed trajectory during its flight. A camera pair is recommended to create multiple samples of image pairs to calculate how the object's depth is calculated from the camera pair[8]. Eqn. 1 gives the value of depth z of the object from the camera pair, given the value of baseline b (distance between optical centers of two cameras), an equal focal length of two cameras f.

$$z = \frac{bf}{p\delta x} \tag{1}$$

Here, p is the pixel size of the camera sensor, and δ_x is the difference between the centroid positions of the detected object of interest, i.e., a shell in our case. Similarly, the calculation of coordinates is to be done for all samples of image pairs. From these points, the flight path of the shell is estimated. The computation required on the first pair of images must be completed before the second sample is captured, and coordinates are calculated. A more practical and feasible technique having an adaptive geometry has been mentioned with multiple camera system[9], with a multi-baseline, multi-resolution camera

setup. The stereo setup varies the baseline and resolution proportionally to depth to obtain a reconstruction in which the depth error is constant. This method is unlike traditional stereo. The error in the depth resolution δz grows quadratically with depth as in Eq. 2, giving a relationship between depth z, depth resolution δz, change in disparity δd, baseline b, and focal length f [10].

$$\delta z = \frac{z^2 \delta d}{bf} \tag{2}$$

We propose an adaptive solution with the specific value of range covered by the shell as a projectile and the speed with which it moves in the air. There are three main parameters (components of the solution), which we address to implement this system to detect and identify the shell's hidden point of origin.

- **The range for imaging:** The last section explained how difficult it is to image a distant world point. The range from where the camera pair has to start imaging can vary between 1 km to 3 km.
- **Speed for imaging:** As discussed in the previous section, the projectile to be detected is expected to move at high speed, high-speed imaging is mandatory to estimate an accurate trajectory.
- **Optimised algorithms:** For object detection and related calculation in stereoscopic images, some application-specific algorithms can be devised from standard algorithms that would meet the computational time requirement of the application.

The proposed system is conceptualized, keeping in mind all the underlying challenges and parameters of interest while designing a system that caters to solutions to those challenges or issues. In the following subsections, critical specifications and their effect on the performance are elaborated.

4. CRITICAL SPECIFICATIONS FOR SYSTEM

A pair of cameras are the core of the system - they gather samples in real-time for further calculations. There are a few vital specifications that define the resolution and range of the system. Sensor size or pixel size, the focal length of the optics, and baseline are three major specifications that define the capability of the stereoscopic imaging system. Imaging sensors with a pixel size of 1 micron are readily available with all kinds of raw data transfer protocols between the camera and the processing platform. Figure 4 shows the relevance of critical parameters in the proposed solution. Two identical cameras (left camera) C_L and (right camera) C_R, are placed parallel to each other with two parallel optical axes O_L and C_R. Both cameras have identical focal lengths f and pixel size p. Both have the same horizontal and vertical Field-of-view, HZ and EL, respectively, and have image planes ABCD and EFGH at a distance z from the cameras. The size of the image plane keeps increasing as we move further from the cameras.

Suppose the object required to be captured is at a distance of z and is imaged by both cameras simultaneously. An object captured is shown in white color in both image planes. where a grid is shown to map pixel array in the camera to image blocks on the target plane. Every target object is accommodated in some number of these image blocks as the target object – in this case, is shown in 12 blocks. For calculation of the depth of any object, it has to be present in the overlapping area between the two FOVs i.e. in rectangle EBCH. We note that the object

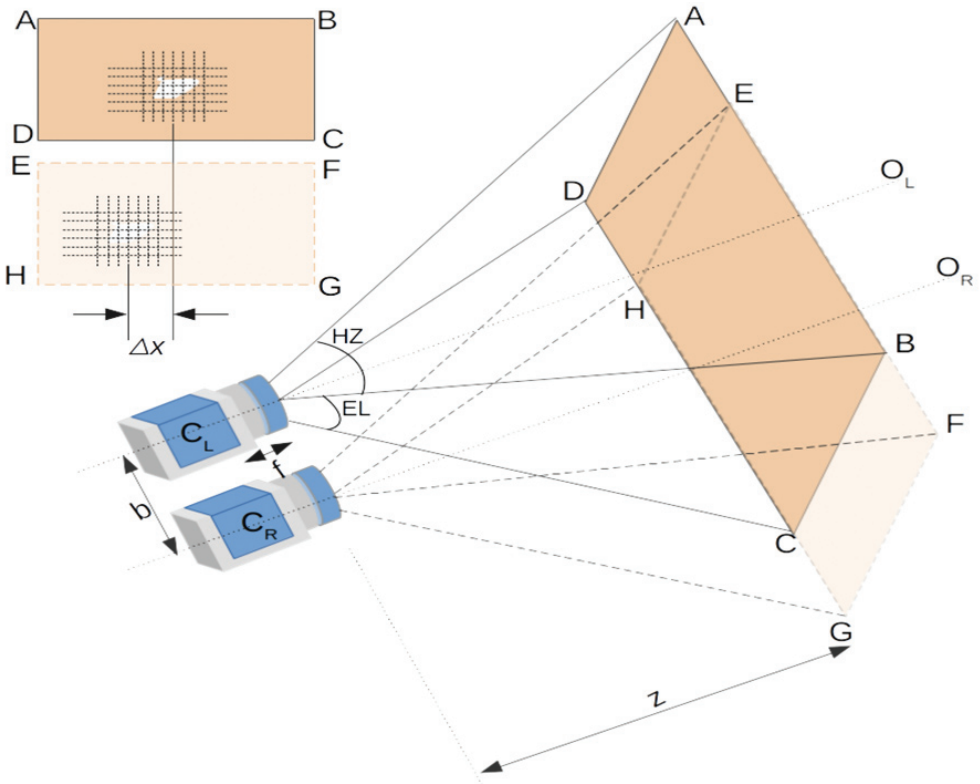

Figure 4. Details of stereoscopic imaging and its parameters.

is captured at a lesser number of column position numbers in the right camera than in the left one. If x_L and x_R are the pixel numbers of the centroid position of the object in the left image plane and the right image plane, then the difference between these two centroid pixels, i.e., $\delta x = x_L - x_R$ decides the distance of the object from the camera pair. The larger its value, the farther the object is, and vice-versa.

4.1 Pixel Size

Pixel size relates to the fine detail which can be extracted from the scene as it resolves the available picture in visually discernible units. For example, a sensor with a 1.0-micron pixel size can resolve the scene better than a sensor with a pixel size of a higher value. It helps in measuring the size of the object more accurately but also in measuring the distance of the object with higher accuracy as it resolves the object with finer details. Although a sensor pair with a lesser pixel size can start detecting the object from a larger distance, there is an increased computational cost.

4.2 Focal Length

Optics which is placed in front of a sensor guides the light on the pixel array or sensor plane. Different values of the focal length of the optics can capture an image of different widths of the physical world. Comparing two different values of focal length, a lesser value of focal length can capture a wider frame and hence detect a threat better when even the coarse direction of incoming artillery threat is unknown. But this reduces the efficacy of the system in detecting the shell from a larger distance, whereas, sensor pair with a larger focal length can give better results in detecting an object from a larger distance at the cost of having a narrower FOV - which can be a liability when detecting the shell moving with high speed. The projectile crosses the FOV sooner, reducing the possibility of sampling the trajectory more often.

4.3 Baseline

There is always a limitation on the distance between two sensors which are a part of the stereoscopic setup. Ideally, both cameras are to be mounted on a single platform with a uniform plane to avoid the need for re-calibration of two cameras. A baseline value of 1m to 10m can be fixed because it will not be economical to have multiple sets of cameras and varied values of baseline.

So, having understood all three critical specifications, and the advantages and disadvantages associated with increasing and decreasing the values of these specifications, we can describe the specifications of pair of cameras in the next sub-section.

5. CUSTOMISATION OF THE PAIR OF CAMERAS

We have stated that the baseline can be varied between a few centimeters to a few meters depending on how stable the mounting platform for the cameras is. We analysed the trade-off between the depth (or distance) of the object resolved and how the image plane having the target object is resolved. As shown in Fig. 5, We propose to have 10m of baseline between cameras which are placed on top of a stable or moving platform e.g., a truck, or other military vehicles – C, a fixed point is the center of the assembly, and two cameras (C_L and C_R) are placed at extreme ends of two arms which have a joint each at A and B hinges respectively. The whole assembly can be stretched to

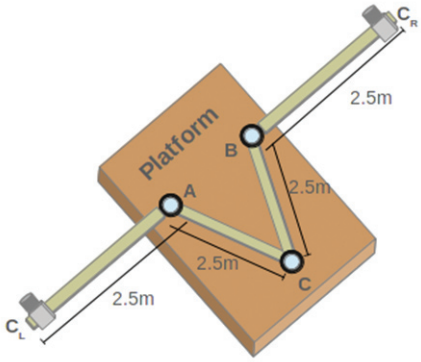

Figure 5. Adjustable mounting assembly for camera pair.

Table 1. Trade-off analysis for different optics for sensors

Depth (m)	f=100mm			f=50mm			f=25mm		
	Disparity (pixel)	Image Plane		Disparity (pixel)	Image Plane		Disparity (pixel)	Image Plane	
		Length (m)	Width (m)		Length (m)	Width (m)		Length (m)	Width (m)
50	5333	2.4	1.8	2666	4.8	3.6	1333	9.6	7.2
100	2666	4.8	3.6	1333	9.6	7.2	666	19.2	14.4
200	1333	9.6	7.2	666	19.2	14.4	333	38.4	28.8
400	666	19.2	14.4	333	38.4	28.8	166	76.8	57.6
600	444	28.8	21.6	222	57.6	43.2	111	115.2	86.4
800	333	38.4	28.8	166	76.8	57.6	83	153.6	115.2
1000	266	48.0	36.0	133	96.0	72.0	66	192.0	144.0
1200	222	57.6	43.2	111	115.2	86.4	55	230.4	172.8
1400	190	67.2	50.4	95	134.4	100.8	47	268.8	201.6
1600	166	76.8	57.6	83	153.6	115.2	41	307.2	230.4
1800	148	86.4	64.8	74	172.8	129.6	37	345.6	259.2
2000	133	96.0	72.0	66	192.0	144.0	33	384.0	288.0

a 10 m baseline and can be folded back around hinges A and B. As A and B are not fixed, the assembly can be folded to a straight line where A and B coincide and fixed fixed-point C at another end.

To have a larger and deeper enough window to sense an incoming high-speed shell, we have analyzed the effects of the varying focal length of the optics. Since disparity in pixels of two images in a stereoscopic system is a reciprocal function of the depth of the object in images, it is impossible to get the constant resolution of depth through this technique. It is evident from Table 1 and this is where the challenge in the design lies. It gives the disparity value in terms of pixels against the depth of the target in the image for different values of the focal length of optics. As the depth resolution of the imaging system varies with the depth, it is evident that the calculation for the depth of the target will yield results with random deviations from the actual depth of the target. For example, in the table, using 100 mm focal length, the distance between 1800 m to 2000 m can be resolved by 5 pixels, which means there will be a maximum error of $\pm$ 20 m . The maximum error is given by $\varepsilon_{max} = \delta z^2 \delta d$, where δz is depth range and δd is the change in disparity across the given range, 1800 m to 2000 m in this case. We try to use linear parts of the different curves for different depths of the target, it makes the design more complex.

Similarly, the image window size is also an important parameter as an incoming artillery shell is coming from a larger distance and it should be in the image window to be detected. As evident from the table, image plane sizes are linear curves as expected for different values of focal lengths. Knowing that the shell will come from a long, distance, higher values of focal lengths should be avoided as they will give a narrower image plane hence reducing the probability of the shell being captured. This leads to a choice among lower focal lengths, and values of 25 mm and 50 mm can be used to extract different benefits. The focal length of 50mm can be used to resolve the depth better with the reasonable size of the image plane at longer distances and a smaller focal length of 25mm can be used to do the same for smaller distances. Hence, we adopted two focal lengths for two pairs of stereoscopic setups. Two shaded regions in the table denote the use of focal lengths of 50mm and 25mm for two different ranges of the depth or distance of the target from sensors.

Table 1 shows a 50 mm focal length to be used between 2000 m distance to 1200 m distance and 25 mm focal length from thereon to the nearest possible point. The maximum error while calculating distance should be 13 m, as per the formula discussed above and the error reduces as the shell is tracked through a smaller distance from the sensor. It is very important to time the capture of two frames at the same time and hence, it makes the job of a centralized processing platform critical. Fast processing of images to extract information on the world coordinates of the target is another responsibility of the processing platform apart from synchronization of the trigger signal to capture images.

6. RESULTS

To sidestep the difficulty of testing the design in an actual combat situation, we worked on a virtual recreation of the digital twin of the actual battlefield terrain using open-source 3D software for computer-generated videos. The videos we created simulated the movement of artillery shells of the same size from a distance. From these generated videos, we applied image processing algorithms on the video to track the shell in flight and calculated the distance of the target from the camera.

6.1 Creating Simulated Videos

We used an open-source tool for creating test videos that simulate the fired shell from the artillery. The tool gives the flexibility to create a terrain of interest[9] and place a camera at any virtual world point to capture the movement of the object or target. Shell with all physical properties was created in the scene and was made to move with the initial velocity in the direction of the location of the camera pair. The tool itself is programmable for all these positions, orientation, velocity, weight, and size. Hence, it helped in creating different videos for a set of cameras placed at a distance equal to the baseline. Figure 6 shows the picture of the terrain created and the movement path of the shell as a projectile from one end of the terrain to another where the source of the shell is completely hidden from another end.

A shell with a 15 cm diameter was simulated as having been fired from one end with velocity components of V_x and V_y equal to 300 ms^{-1} and 100 ms^{-1}. The shell was 'fired' from the right side of Fig. 6 and the camera system is placed towards the left side of the frame with the shell coming towards it. The camera was to measure or locate points of the shell's trajectory to extrapolate it to point of origin. We chose the specifications of the camera to match an existing camera, i.e., the Basler *DAA1280*-54 µm was emulated. Pixel size was chosen to be 3.75 microns and the resolution of the image of each camera was set at 1280x960 pixels. Two cameras (for stereoscopic setup) were placed 10 m apart on the same plane to create just an ideal stereoscope. Videos from both cameras were captured

Figure 6. Shell traveling after being fired from artillery.

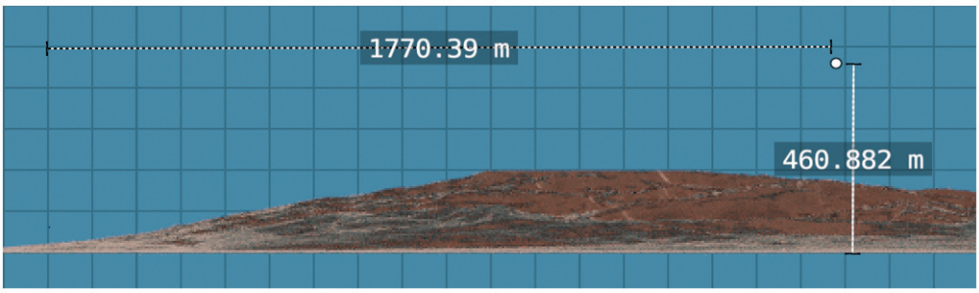

Figure 7. Point coordinates measured manually.

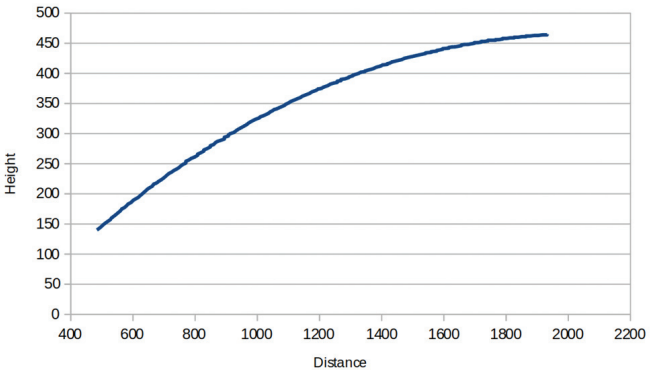

Figure 8. Trajectory of the shell with manually measured points.

at 24 *fps* while the shell was moving. Those captured videos are *exactly* synchronized for all frames. This means that there is no delay or gap in capturing the frame from either camera for each frame. This is crucial because a high-speed moving object will give erroneous results for its coordinates if two cameras capture at two different instances of time, whatever smaller time gap it might have.

The rendering software used has features where the location of the shell is recorded for each frame during flight, as shown in Fig. 7, where the shell represented by a white small circle is recorded to be at [1770 m, 460 m] for [distance, height]. Similarly, Fig. 8 plots the movement of the shell in the form of its height from the ground and distance from the camera for all captured points.

Through this exercise, we created an ideal test case for further processing on videos to calculate world coordinates and work on the shell's trajectory as a projectile.

6.2 Tracking Algorithm

There are broadly two different approaches for finding out the required information from the sets of videos with respect to the concerned problem. The first approach is to detect the object of interest, i.e., the shell in each image, and then find out its center of geometry in each frame. This has to be executed parallel to another image of the stereoscope. The difference between pixel numbers between geometrical centers of the target detected in two images leads to all calculations which find out values of world coordinates of the target shell. Similarly, the process is repeated for each frame to draw a trajectory. Another approach is to track the movement of any object in the video which has a relatively stable background. It has few advantages over the first approach as it has a higher probability of finding the object of interest in a smaller zone in the image given the object's position in the previous frame. Once the tracked object's boundary is finalized, the geometrical center of the object is calculated as discussed in the first approach and hence other calculations are executed consecutively.

There are many proven and published techniques for tracking the movement of the object(s) in the video but choosing the most optimum one for the problem concerned is desired. There are background subtraction techniques[10-11] that require a stable background and are not suitable for dynamic background. Then, there is a technique that works using pixel-to-pixel differencing between consecutive frames[12]. It is used to detect every minute movement, but it is processing intensive and can create a lot of uncertainties in deciding the boundaries of objects for high-speed movement. Then there are techniques for estimating optical flow in the image[13], which are resistant to camera instability but are computationally so complex that they find few applications in scenarios where real-time response is desired. There are certain statistical methods[14], which tend to classify each pixel or group of pixels as foreground or background. There is a technique that makes the algorithm insensitive to changes in image intensity during physical or environmental changes in the background scene[15]. These methods use disparity in RGB color space for all pixels. Still, this technique again is too complex for real-time applications like the one being addressed in this paper.

As our application does not require motion detection for a long time, it can be assumed to be insensitive to the change in intensity and hence can be worked upon on the gray color model. There is a technique used by researchers for tracking humans and vehicles, both slow and fast, and it is very low on computational cost. This technique is called Differencing and Summing Technique[16], and we applied it to the videos created through the rendering tool. Figure 9 shows a random frame from the video captured by one of the cameras and shows an encircled small black color shell in the sky, whereas Fig. 10 shows the shell detected and tracked in frames (Frame numbers 10, 80, and 150 in the video). Snapshots of the zoomed images have been displayed in the figure for better clarity of vision.

Figure 9. Frame in the video without tracking.

Figure 10. Tracking of the shell for different frames during movement.

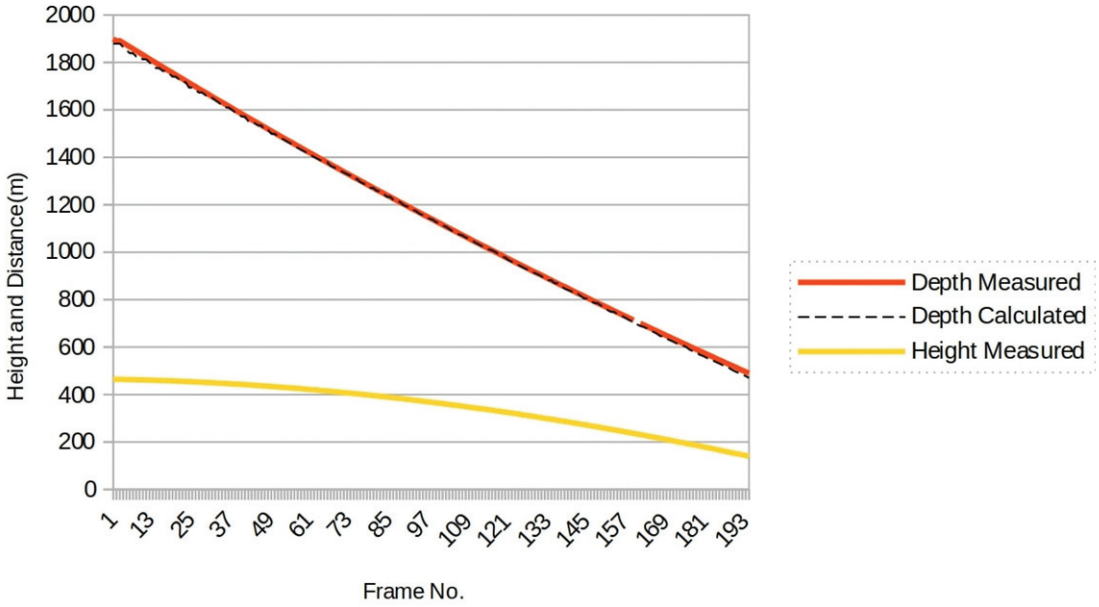

Figure 11. Results chart for captured shell positions.

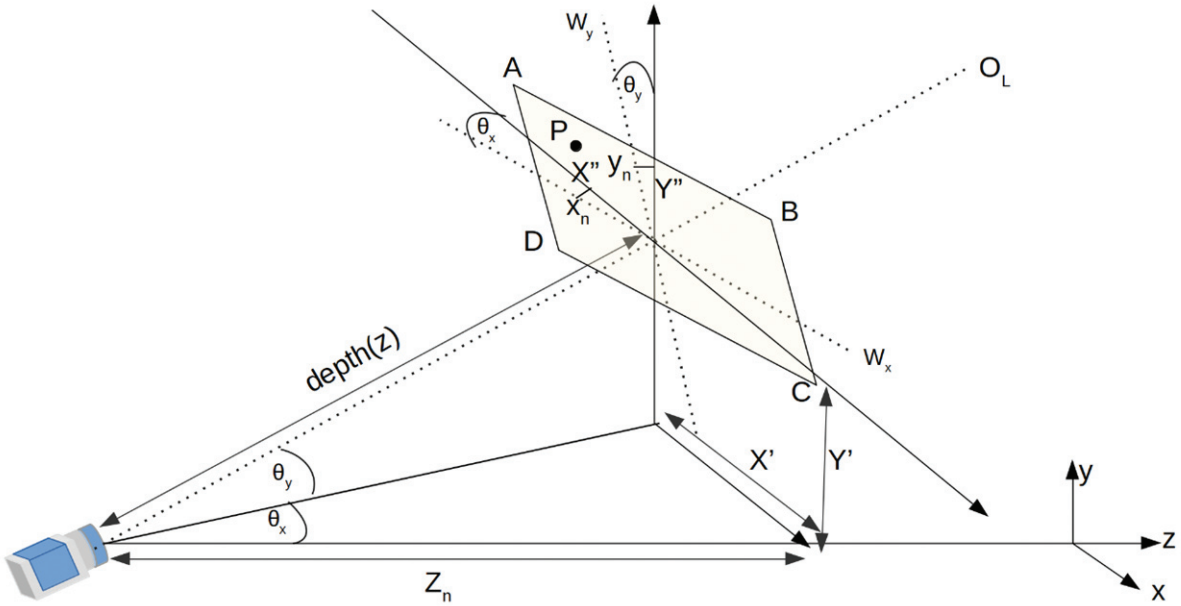

Figure 12. Diagram showing how X-Y coordinates are estimated.

After calculating the value of Z_n (depth) of the shell for each captured frame it was observed that all errors were within 20m for the whole tracking range. Figure 11 gives the measured depth of the shell across video frames (represented by dots), in contrast, two other plots give the depth and height (Orange curve) of the shell (manually recorded from the rendering tool) across all video frames.

6.3 Calculations of Relative Coordinates

As given in Fig. 12, P is the centroid of the tracked object with coordinates (X_n, Y_n, Z_n). It is mapped to the left camera at (x_n, y_n). X, Y, and Z axes are shown to have a 3D perspective of the scene and how all the angles and coordinates are related. O_L is the optical axis of the left camera and cuts the window ABCD (for the nth frame) at the center. W_x and W_y are two

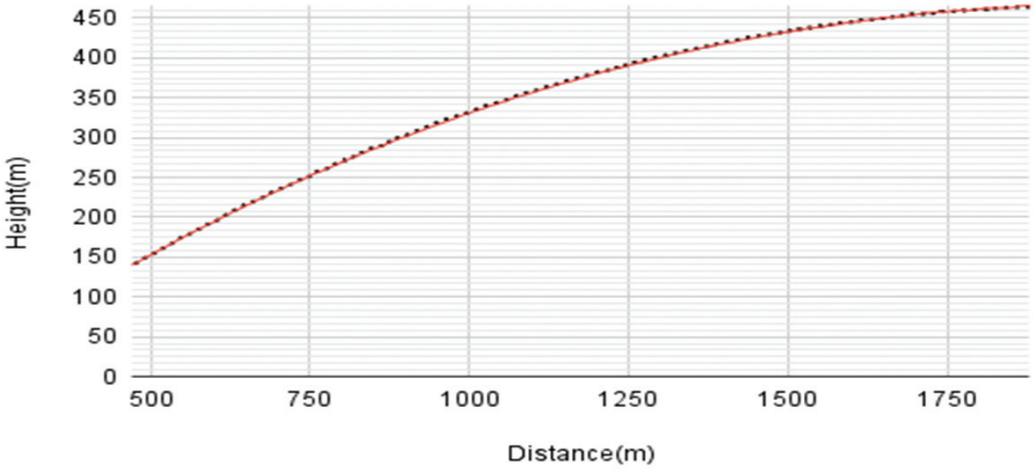

Figure 13. Results for calculation of the height of the shell.

perpendicular axes of the plane of the captured scene and make angles θ_x and θ_y with the X and Y axes of the world coordinate system. Z_n gives the relative depth of the shell from the camera for n^{th} frame and is given by $z\cos\theta_x \cos\theta_y$. Once Z_n is calculated, the calculation of other two relative coordinates, X_n and Y_n for all captured points is carried out using following equations:

$$Y_n = Y' + Y'' \tag{3}$$

$$Y' = Z_n \tan\theta_y \tag{4}$$

$$Y'' = \frac{Z_n p(y_n - y_c)\cos\theta_y}{f} \tag{5}$$

where, p is the pixel size (3.75~μm in this case), f is the focal length of the optics (50 mm and 25 mm in this case), x_c and y_c are pixel numbers at center of the sensor plane for both x and y directions (640 and 480 in this case) and (x_n, y_n) is the position of the geometric center of image of detected shell in the n^{th} video frame.

Similarly, for X_n,

$$X_n = X' + X'' \tag{6}$$

$$X' = Z_n \tan\theta_x \tag{7}$$

$$X'' = \frac{Z_n p(x_n - x_c)\cos\theta_x}{f} \tag{8}$$

Based on these formulae, calculations were carried out for the estimated height of the detected shell for a full range of its tracking in consecutive 194 frames as the shell traveled from a distance of 1900 m to almost 400 m. Results were compared with the manual measurements done over the rendering tool and all results for the height were within a 2 m error. Figure 13 gives the plot of the actual movement of the shell across distance and height (continuous line) versus the calculated height of the shell for all frames (dotted line). There is excellent agreement with negligible error in the two plots, measured and actual.

7. CONCLUSION

Through the simulations of a combat scenario and the implementation of proven techniques over simulated videos, we could demonstrate the feasibility of the concept for a realizable system. The engineering aspects for the realization of actual hardware after the proof of concept have also been taken into consideration. Results for the measurement of relative coordinates of the high-speed shell at certain instants of time are verified with those of simulated moving shells fired from a projectile-emitter in the video. Results of the calculation of the position of shells were effectively verified on two different video pairs having focal lengths of 25 mm and 50 mm for two sections of the flight path. In practical situation there will be occlusion, rain, poor visibility to challenge the sensitivity of the algorithm and it is comprehensive work. There is a lot of scope for further work and estimating the exact location of the artillery gun using such an inexpensive visual technique will be a challenging job, but it may eventually lead to realizing a camera-based counter-battery fire system. Similarly, interpolation and extrapolation using multiple mathematical tools to extend the trajectory information to Point of Origin is a section of research in itself with respect to the problem being addressed.

REFERENCES

1. Woodridge, K. & Banahan, C.P. Dynamic detection capability of a mobile bistatic weapons locating radar. *In* Proceedings of the 2003 IEEE Radar Conference (Cat. No. 03CH37474), May 2003, pp. 179–184. doi: 10.1109/NRC.2003.1203399.
2. Khudov, H.; Yuzova, I.; Lisohorskyi, B.; Solomonenko, Y.; Mykus, S.; Irkha, A.; Onishchuk, V.; Sukonko, S.; Semiv, G. & Bondarenko, S. Development of methods for determining the coordinates of firing positions of roving mortars by a network of counter-battery radars. *EUREKA Phys. Eng.*, 2021, **3**(3). doi: 10.21303/2461-4262.2021.001821.
3. Holovan, V.; Gerasimov, V.; Holovan, A. & Maslich, N. Real condition and prospects of development of the radar stations of the counter battery fighting. *Collect. Sci. Works Odesa Mil. Acad.*, 2019, **1**, 30–40. doi: 10.37129/2313-7509.2019.12.1.30-40.
4. Gural, P.S. A new method of meteor trajectory determination applied to multiple unsynchronized video cameras. *Meteorit. Planet. Sci.*, 2012, **47**(9), 1405-1418. doi: 10.1111/j.1945-5100.2012.01402.x.
5. Robinson, G. & Robinson, I. Radar speed gun true velocity measurements of sports-balls in flight: Application to

tennis. *Phys. Scr.*, 2016, **91**(2), 023008.
doi: 10.1088/0031-8949/91/2/023008.
6. Bolonkin, A. Long distance bullets and shells. *Int. J. Aerosp. Sci.* 2013, **2**(2), 29–36.
doi: 10.5923/j.aerospace.20130202.01
7. Rong, Z.; Yi, Z.; Jikun, Z. & Haiying, H. Research on the artillery shell motion parameters automatic detection technology based on image processing. *Procedia Comput. Sci.*, 2015, **52**, 1171–1178.
doi: 10.1016/j.procs.2015.05.154.
8. Scharstein, D. Szeliski, R. & Zabih, R. A taxonomy and evaluation of dense two-frame stereo correspondence algorithms. *In* Proceedings IEEE Workshop on Stereo and Multi-Baseline Vision (SMBV 2001), Dec. 2001, pp. 131–140.
doi: 10.1109/SMBV.2001.988771.
9. Frahm, D.J.M.; Mordohai, P. & Pollefeys, M. Variable baseline/resolution stereo. *In* 2008 IEEE Conf. Comput. Vis. Pattern Recognit., pp. 1–8, 2008,
doi: 10.1109/CVPR.2008.4587671.
10. Kytö, M.; Nuutinen, M. & Oittinen, P. Method for measuring stereo camera depth accuracy based on stereoscopic vision., 2011, **7864**, 1.
doi: 10.1117/12.872015.
11. d'Oliveira, R.B.D.; & Apolinário Jr, A.L. Procedural planetary multi-resolution terrain generation for games. arXiv, Mar. 13, 2018.
doi: 10.48550/arXiv.1803.04612.
12. Migdal, J. & Grimson, W. Background subtraction using markov thresholds., 2005, **65**.
doi: 10.1109/ACVMOT.2005.33.
13. Pai, C.J.; Tyan, H.R.; Liang, Y.M.; Liao, H.Y. M. & Chen, S.W. Pedestrian detection and tracking at crossroads. *Pattern Recognit.*, 2004, **37**(5), 1025–1034.
doi: 10.1016/j.patcog.2003.10.005.
14. Thome, N. & Miguet, S. A robust appearance model for tracking human motions. *In* IEEE Conference on Advanced Video and Signal Based Surveillance, September 2005, pp. 528–533.
doi: 10.1109/AVSS.2005.1577324.
15. Denman, S.; Chandran, V. & Sridharan, S. Adaptive optical flow for person tracking in Digital Image Computing: Techniques and Applications (DICTA'05), Dec. 2005, pp. 8.
doi: 10.1109/DICTA.2005.11.
16. Allili, M.; Bouguila, N. & Ziou, D. A robust video foreground segmentation by using generalised gaussian mixture modeling., 2007, 509.
doi: 10.1109/CRV.2007.7.
17. Murali, S. & Girisha, R. Segmentation of motion objects from surveillance video sequences using temporal differencing combined with multiple correlation. *In* 2009 Sixth IEEE International Conference on Advanced Video and Signal Based Surveillance, Sep. 2009, pp. 472–477.
doi: 10.1109/AVSS.2009.15.
18. Thapa, G.; Sharma, K. & Ghose, M. Moving object detection and segmentation using frame differencing and summing technique. *Int. J. Comput. Appl.*, 2014, **102**, 20–25.
doi: 10.5120/17828-8647.

ACKNOWLEDGMENT

This research work originated from the idea of Subrat Kar about developing a visual counter-battery system that can replace Radar based counter-battery systems in artillery combat.

CONTRIBUTORS

Mr Manoj Sharma is a DRDO scientist. His areas of research include: Optoelectronic sensors and systems for defence applications.
His contributions to the proposed work include: Simulations, generation of videos, figuring out specifications of components to implement the idea, and applying image processing algorithms to achieve the result.

Mr Subrat Kar is a Professor of Electrical Engineering at IIT Delhi. His research interests are optics, embedded telecom systems, telecom transmission and switching, automotive networks, deep space communications, and biomedical instrumentation. His contribution to the proposed paper includes the original idea of a multiple-camera-based system to replace bulkier and costly radar-based counter-battery systems in artillery combat. He guided the main author all through the implementation of the idea.